communications
earth & environment

ARTICLE

https://doi.org/10.1038/s43247-022-00405-w OPEN

Societal drought vulnerability and the Syrian climate-conflict nexus are better explained by agriculture than meteorology

Lina Eklund[1,2✉], Ole Magnus Theisen[3], Matthias Baumann[4], Andreas Forø Tollefsen[5], Tobias Kuemmerle[4,6] & Jonas Østergaard Nielsen[4,6]

Droughts are often suspected to increase the risk of violent conflict through agricultural production shocks, and existing studies often explore these links through meteorological proxies. In Syria, an alleged agricultural collapse caused by drought is assumed to have contributed to increased migration and the conflict outbreak in 2011. Here we use satellite derived cropland and climate data to study land use dynamics in relation to drought and conflict in Syria. We show that claims of an agricultural collapse cannot be substantiated as croplands saw a fast recovery after the 2007–2009 drought. Our study highlights the importance of considering land-use dynamics for understanding linkages between meteorological droughts, agricultural impacts, migration and conflict. Furthermore, our results suggest that the influential drought-migration-conflict narrative for Syria needs to be reexamined, with implications for wider discussions of how climate change might alter conflict risk.

[1] Department of Physical Geography and Ecosystem Science, Lund University, Sölvegatan 12, 223 62 Lund, Sweden. [2] Centre for Advanced Middle Eastern Studies, Lund University, Finngatan 16, 22362 Lund, Sweden. [3] Department of Sociology and Political science, Norwegian University of Science and Technology, Dragvoll, 7491 Trondheim, Norway. [4] Geography Department, Humboldt-Universität zu Berlin, Unter den Linden 6, 10099 Berlin, Germany. [5] Peace Research Institute Oslo (PRIO), PO Box 9229 Grønland, NO-0134 Oslo, Norway. [6] Integrative Research Institute on Transformations of Human-Environment Systems (IRI THESys), Humboldt-Universität zu Berlin, Unter den Linden 6, 10099 Berlin, Germany. ✉email: lina.eklund@nateko.lu.se

The relationship between climate change and conflict has received much attention in research and policy alike[1,2]. Weather extremes, such as meteorological droughts, have been found to sometimes coincide with armed conflict outbreaks, suggesting a potential causal mechanism between the two[3,4]. Agricultural production shocks, often with subsequent migration, constitute the most commonly suggested mechanism linking climate to violent conflict[5,6]. Yet, sparse or unreliable sub-national data on agricultural yields and cropping patterns for countries with high conflict risk[7] has largely prevented scrutiny of the assumption that weather extremes lead to increased agricultural vulnerability in conflict studies[4,5,8]. With a few notable exceptions[9–11] the majority of studies have solely relied on meteorological data and assume that these indicate widespread crop failure, or even agricultural collapse, arguably contributing to a lack of overall consensus on the relationship between climate and conflict[5,12–22].

Studies and media reports have, to varying extents, linked the 2011 political protests in Syria, and the ensuing civil war, to the severe drought that affected the Middle East between 2007 and 2009[23–25]. The reasons behind the Syrian uprising are complex and manifold. They include increasing unemployment and poverty levels, corruption, repression and police brutality, injustice, a growing rural-urban divide, and a lack of political freedom[26–28]. Even though there were many causes of the conflict, the drought has received much attention, either as a trigger of the conflict or as a major factor contributing to it[29]. Several scholars have argued that the drought caused a collapse in Syria's agricultural system[24,30,31], with subsequent widespread rural-urban migration[32,33]. This reportedly placed much strain on Syrian cities and, in turn, contributed to the Syrian uprising in 2011[24,30,31,33,34] (Fig. 1B). Although plausible, the evidence for such a causal chain is mainly anecdotal or based on events that coincide in time, yet little data exists to back up this drought-migration-conflict nexus[28,29,35,36]. There is also evidence that the unrest concentrated largely in areas with less severe drought impacts[34], and that migrants were generally not linked to the protests[28,36,37]. Moreover, it is unclear whether the drought induced a qualitative shift in the agricultural system (i.e. a collapse) or if it, despite its undeniable severe impact, rather constituted a shock from which the agricultural system recovered (Fig. 1B, C).

In Syria, groundwater depletion and land salinization were substantial more than a decade before the 2007–2009 drought[28,35,38]. A suggested reason behind this degradation is the neoliberal restructuring of the economy since 2000, causing underinvestment in agricultural infrastructure combined with bad environmental governance and an over-exploitation of water resources[26,35,39]. In particular, the four northeastern governorates (Fig. 1A), where the 2007–2009 drought was the harshest, were subject to the most aggressive and, arguably, unsustainable agricultural expansion[38]. Farmers experienced additional strains in May 2008 and May 2009 when the government removed fuel subsidies, causing pumping of irrigation water to become more than three times more expensive[40], and fertilizer subsidies respectively[26,40]. These cuts may have increased agricultural sensitivity to meteorological drought in the subsequent period, particularly in areas relying on diesel-pump irrigation. In 2010, a yellow rust outbreak reportedly led to 300,000 hectares of wheat becoming un-harvestable[40]. How these factors have contributed to the alleged agricultural collapse preceding the conflict outbreak in Syria remains weakly understood.

The term agricultural collapse is itself problematic and has been used loosely in the literature. Assessing whether or not agricultural collapse has occurred requires a stringent definition. On a general level, agricultural collapse can be defined as a breakdown of agricultural production that leads to a fundamental shift in the agricultural system[41]. This resonates well with notions of state or regime shifts in social-ecological systems, where a collapse should meet four criteria: (i) abruptness of factor driving change, (ii) substantial loss in a state variable, and (iii) persistence of this loss, leading eventually to (iv) a structural change to the system[41–43]. Assessing agriculture through the lens of regime shifts thus means that a collapse involves change that occurs quickly in comparison with regeneration times (i), and these changes should be much more severe than changes caused by previous similar events (ii). The consequences of a collapse need to be lasting (iii), and include

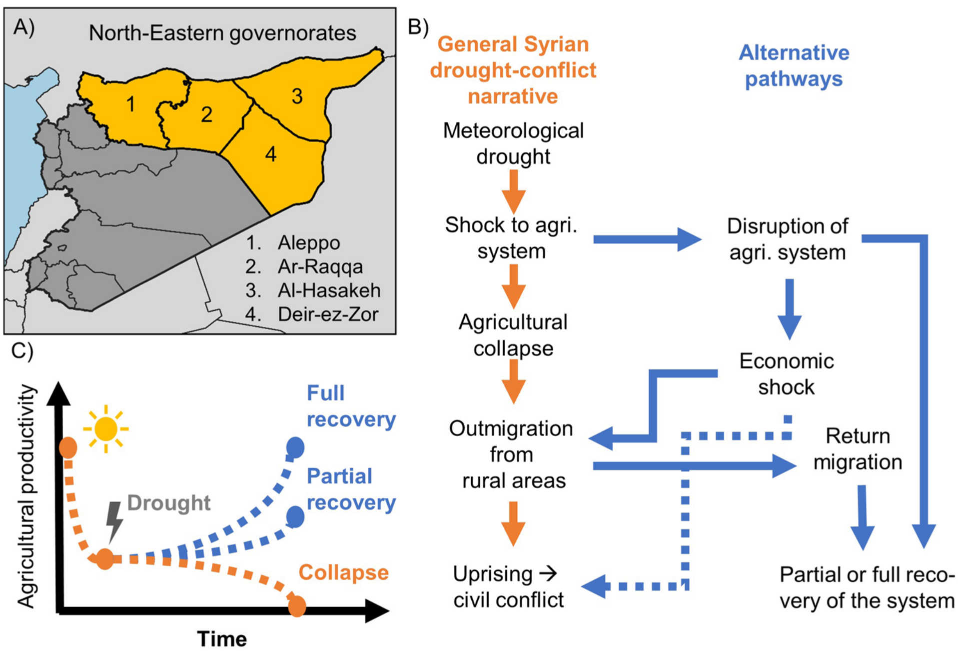

Fig. 1 Situating the study geographically and conceptually. A Study area, including the four North-Eastern governorates. **B** Conceptual model of the Syrian drought-conflict narrative and some alternative pathways discussed in this paper. **C** Conceptual chart of different drought outcomes on the agricultural system.

the disappearance of key actors, system components, and interactions (iv).

Here we discuss the extent to which the 2007–09 Middle East drought produced an agricultural collapse, subsequent migration, and indirectly contributed to the conflict in Syria. Studies of the Syrian drought follow the general approach in the literature—relying largely on meteorological data[23–25,34] and leaving the crucial question of how the drought-affected agricultural activity and productivity unanswered. As a result, the question of whether or not the drought has contributed to, or even triggered, the Syrian conflict continues to be debated and has reached a dead end—with diverging interpretations of the scant evidence that exists on the agricultural decline and migration[29,34,36,44–46]. We here argue that there is an urgent need to move beyond weather data towards directly observing changes in agricultural activity in order to better understand the mechanisms linking drought and conflict.

Focusing on the Syrian conflict, the droughts preceding it and the claim of an agricultural collapse, we aim to fill this gap by studying satellite-based time series data on cropland dynamics covering the pre- and early-conflict period in Syria. Specifically, we map active and fallow croplands, and measure the share of fallow land (hereafter "fallowness") for each year between 2000 and 2016. Croplands are an excellent indicator of the productivity of the agricultural system as a whole, as croplands provide staple crops to local populations as well as the majority of fodder for livestock in the dry season[47]. FAOSTAT data shows that cereals (mainly wheat) was the most common commodity produced in Syria during the period of interest[48]. Furthermore, croplands in dry regions can be relatively easily monitored using satellite images, in contrast to the livestock sector, where grazed and ungrazed areas cannot be easily separated, and because detailed livestock data are not available. We also include national FAOSTAT-data on livestock numbers and a brief analysis in the SI (Supplementary Discussion 1, Supplementary Fig. 1).

Using these analyses, we address the overarching research question: How did the 2007–2009 drought affect the Syrian agricultural system right before the outbreak of the Syrian civil war in 2011?

Three subquestions structure the paper:

1. What were the effects of climate variability on agriculture in Syria, as approximated through changes in cropland extent?
2. How did the vulnerability of Syria's agricultural system to drought and dryness change between 2000 and 2016?
3. Do the observed cropland dynamics fit the criteria of an agricultural collapse?

We use the concept of drought to specifically address the drought periods in the early and late 2000s, and "dryness" to refer to the combined meteorological (precipitation and temperature) conditions over the October-March growing season of each year. Our univariate spatio-temporal analysis shows a sharp increase in fallowness in 2008, followed by a partial recovery by 2009, and a near-full recovery by 2010. A subsequent statistical analysis finds a causal relationship between dryness and fallowness, and some support for increased drought sensitivity during the post-drought period, but this can only to a limited extent be attributed to irrigation dependence and local violence.

Results and Discussion

Changes in agricultural activity, 2000–2016. As a proxy for agricultural productivity, we used cropland maps derived through remote sensing (see Methods, Supplementary Fig. 2 and Supplementary Tables 1–5). Our first major finding is that the extent of fallow cropland in Syria varied widely over the whole period, with a median of 21% of cropland being fallow each year (Fig. 2A). The years 2000 and 2008 stand out, with around half of the cropland laying inactive. The years 2010 and 2013 had low levels of fallowness, with around 90% of cropland actively being cultivated. The years 2006 and 2007, which are sometimes described as drought years[23,24,26], also had a below-median fallowness with only 15% and 16%, respectively. Fallowness patterns largely followed dryness patterns, as measured by the 6-month Standard Precipitation-Evaporation Index (SPEI6, Fig. 2A). At the peak of the drought (in 2008), we recorded a high level of fallowness (50%) compared to previous years (around 15%), yet, as the dryness decreased in 2009, substantially less fallowness occurred (25%) (Fig. 2A).

The high fallowness rates in 2008 struck all of Syria's cropland regions, but effects were particularly pronounced in the primary grain-producing area of northeastern Syria (Al-Hassakeh province), where most agricultural land, independent of cropping frequency, was left fallow (Fig. 2B, C). The partial recovery in 2009 appeared in areas where higher cropping frequencies were more common, still leaving many less frequently cropped and marginal areas fallow in the northeast (Fig. 2B, C)—the areas that had lately seen the most aggressive expansion. This indicates that cultivation was prioritized in areas with high-intensity farming. Very little land was permanently fallow after the drought. Only 113 km^2 (0.5% of all normally active cropland) of the cropland actively cultivated in the years preceding the drought (2006 and/or 2007) showed indications of abandonment (i.e. left fallow for all the subsequent five years, 2008–2012). In terms of area cropped, Syria's agriculture recovered from the 2007–2009 drought. While fine-scale data on grazing or livestock dynamics are not available for the time period we studied, national-scale livestock numbers confirm the pattern found here for croplands, with livestock numbers declining during the drought, but recovering thereafter (see Supplementary Discussion 1 and Supplementary Fig. 1).

Drought effects on fallowness and vulnerability. Did the agricultural system become more vulnerable to meteorological disturbances after the 2007–2009 drought? In order to test this, we ran a host of spatial fixed-effect models of the effect of dryness (below-normal water availability as measured by SPEI6) on fallowness with marginal effects depicted in Fig. 3. This allowed us to discern whether agricultural sensitivity to dryness increased after the drought, after the subsidy cuts (in 2008 and 2009), and after the conflict outbreak. We also assessed whether increases in sensitivity were more pronounced in the northeastern governorates and in areas reliant on irrigation—areas affected both by drought and the removal of fuel subsidies. As conflict is often argued to increase vulnerability, we also tested whether local violence enhanced sensitivity to drought.

Overall, drier periods coincided with stronger cropland declines. One standard deviation below normal SPEI increased fallowness by approximately 11–12% for the full period (2000–2016), confirming the pattern shown in Fig. 2A. Regarding increasing sensitivity over time, we found that for the pre-drought and pre-subsidy-cuts period (2000–07), one standard deviation drop in SPEI increased fallowness by approximately 7–8% compared to a 13–18% increase for the 2008–2016 period (Fig. 3). Although not statistically significant, we found a considerably higher sensitivity to dryness in the post-drought period, in particular for the later conflict years (2013–2016). For the latter, one standard deviation drop in SPEI resulted in approximately 17% (black) and 22% (blue) increase in fallowness, representing more than double the effect for 2000–2007 (Fig. 3 and Supplementary Tables 7 and 8). Nevertheless, the enhanced

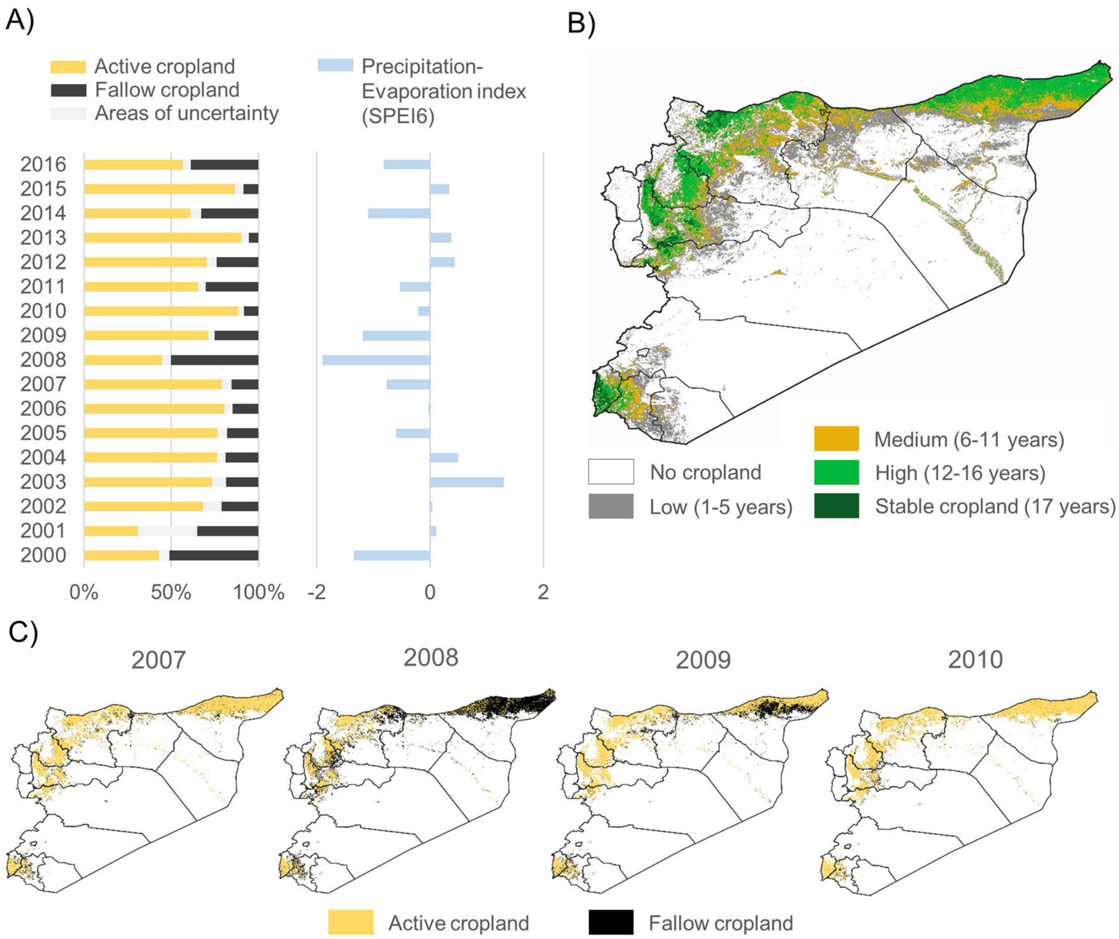

Fig. 2 Fallow land extent before and during the outbreak of the Syrian civil war. A Relative extent of active and fallow cropland between 2000 and 2016 (yellow and black bars). Bright grey bars (between yellow and black) represent areas of uncertainty based on our accuracy assessment. Blue bars: annual 6 month Standard Precipitation-Evaporation Index (SPEI6, based on CRU v. 3.4.4) for Syria 2000–2016, **B** cropping frequency in Syria 2000–2016, **C** active cropland and fallow cropland in the years preceding the conflict outbreak (2007-2010). Data for the figure is provided in Supplementary Data 1.

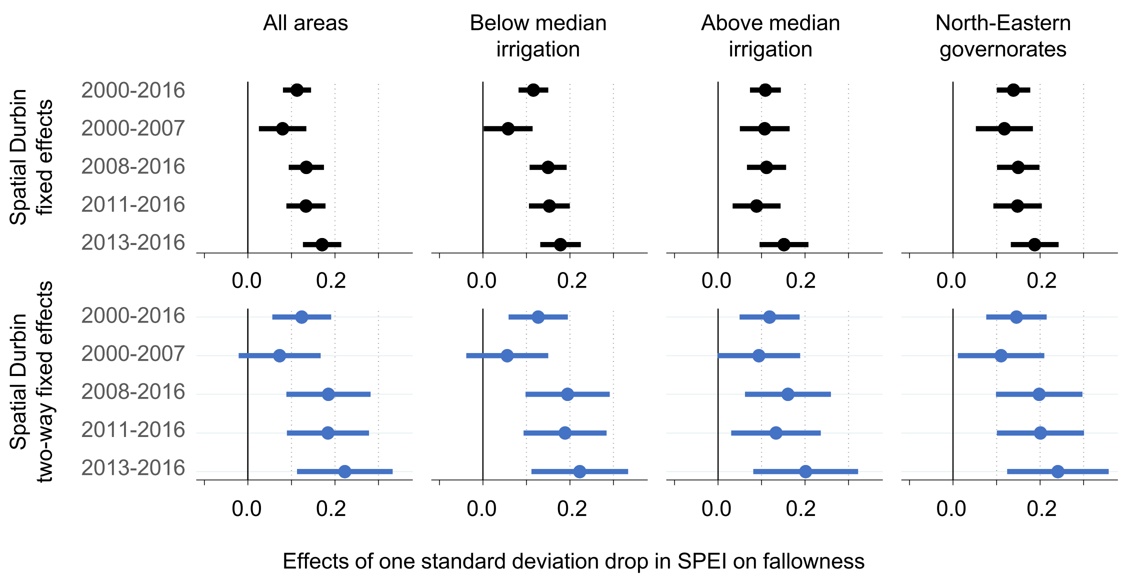

Fig. 3 Dryness effects on fallowness in different contexts and time periods. Marginal effects of sensitivity to dryness on extent of fallowness using spatial Durbin fixed effects (black) and spatial Durbin two-way fixed effects (blue) during different time-periods and within different areas. Whiskers represent 95% confidence intervals. Supplementary Tables 7–18 present the parameters and full results for all models. Data for the figure is provided in Supplementary Data 2.

sensititivity to drought during the conflict years can only to a small extent be safely attributed to violence proximate to croplands. Although the quick recovery of cropland after the 2007–2009 drought refutes the assumption of a collapse, we found indications of an overall structural shift in terms of increasing vulnerability to drought in our data, in particular for the conflict years.

We find little support for the argument that irrigated areas experienced increased vulnerability after the subsidy cuts. Our results instead show that both irrigated and rain-fed areas were affected and that areas with below-median irrigation levels experienced a slightly larger increase in vulnerability (Fig. 3 and Supplementary Tables 9 and 10). Likewise, our separate analyses of the four North-Eastern governorates largely resembled the overall results (Fig. 3 and Supplementary Tables 11 and 12). We find only some indications for local violence enhancing vulnerability to drought (Supplementary Table 19). Our data therefore reflects a pattern expected for an agricultural system that is adapted to drought periods and thus has the ability to bounce back after such shocks. However, after 2008, the drought vulnerability increased, suggesting a structural shift of the agricultural systems, which could increase the risk of future collapse.

Agricultural collapse and permanent outmigration? Drought-induced agricultural collapse causing widespread rural outmigration is a central premise in the climate-conflict argument related to the Syrian conflict. We assess this claim through the lens of social-ecological systems, using the collapse criteria put forward by Cumming and Peterson[42]: (i) abruptness, (ii) substantial loss, (iii) persistence, and (iv) structural change. We find that the drought-related changes to the agricultural system were indeed abrupt (i), as we recorded a sudden three-fold increase in fallowness from 16% in 2007 to 50% in 2008, likely due to widespread crop failures. Whether this represents a substantial loss compared to previous perturbations (ii) is less clear, but appears unlikely as our data indicate that the drought period around the year 2008 led to similar levels of fallowness as the one in the early 2000s, with 51% fallowness in 2000 and a complete recovery in 2002 (21% fallowness). After the 2008–2009 decline, the active cropland extent did bounce back to high levels in 2010. Consequently, the drought-related increase in fallowness was not persistent, refuting criteria (iii). Only a very small area (0.5% of cropland) showed long-term fallowness after 2008 and, in 2010, the fallowness levels were below median. As for the structural change criteria (iv), we find some evidence for the agricultural system becoming more vulnerable to dryness after the drought. However, we suggest a mix of subsidy cuts, unsustainable agricultural practices, and to some extent local violence, are likely more important than drought for this change (see Supplementary Table 19 for effects of violence on drought sensitivity). While we acknowledge that cropland dynamics may not reflect the agricultural system as a whole, it is an important indicator considering the importance of wheat as a staple crop[49]. The fact that livestock numbers follow a pattern similar to cropland dynamics further strengthens our conclusion that this was a temporary decline rather than an agricultural collapse.

Comparing the periods 2000–2007 and 2008–2016, we find that slightly more cropland was left fallow during the latter period. Our analysis suggests that a major reason for this is that the latter period includes drier years, even if excluding the 2008–2009 drought. The latter period may also include the effects of fuel and fertilizer subsidy cuts, that occurred in 2008 and 2009 and likely increased the agricultural system's vulnerability. Furthermore, and arguably more importantly, the latter period includes the outbreak of the armed conflict in Syria, which caused a humanitarian crisis with outmigration and displacement, and also affected infrastructure and government support for vulnerable farmers. Our statistical analysis reflects this, showing an increasing vulnerability to dryness between 2013 and 2016, although there is only weak evidence of an effect of local violence on increased vulnerability. A fourth factor that may be reflected in the fallowness data for 2011 and 2012 (31% and 34% respectively) is the yellow rust outbreak of 2010, in which 300,000 hectares of wheat were affected, representing 13% of the mapped croplands[40]. This estimate, however, indicates that the majority of active cropland in 2010 yielded usable harvests, and only a small part of it had to be discarded due to yellow rust. Our data show very low levels of fallowness in 2013 and 2015, suggesting that agricultural activity was maintained, despite the drastic shock that armed conflict entailed on top of the drought, pest outbreaks and subsidy cuts.

Migration is a supposed key link in the causal chain between drought, agricultural abandonment, and elevated conflict risk. Research on climate stress and migration show that droughts may either increase or decrease migration depending on the socio-economic and political characteristics of exposed communities[50]. Agriculture is considered an important link between climate stress and migration, where migration becomes an adaptation option in the absence of other options, when agricultural livelihoods are compromised[51]. Perceived climate stress has also been identified as a factor influencing migration[52]. While data for Syria on migration are scant and uncertain, migration in Syria likely surged during the drought years[29], as farmers and farm workers (temporarily) migrated to cities or other areas for jobs[37]. Yet, our finding that most of the cropland was again actively used in 2010 indicates that farmers and farm workers either returned, or that lands were used by others by 2010. Reported coping strategies facing the drought in Syria includes distress sales of household assets, loans, reduced food intakes (resulting in malnutrition), and internal or international migration[53]. Thus, the drought may have caused deeper changes to the socio-economic system, which are impossible to infer from our satellite-based assessment of cropland dynamics alone. However, considering the previous mobility of the rural population in Syria and the reported temporary migration of rural households in connection with the drought[37], temporary migration of one or several household members in 2009, after a severe crop failure in 2008, and a return in 2010 is a plausible explanation. The narrative of widespread permanent rural-urban migration (or "mass migration") of farming families leading to long-term cropland abandonment is, in contrast, not supported by our findings.

Conclusion: a better understanding of the drought-agriculture-conflict nexus

The Syrian case provides useful lessons for the climate-conflict community as a whole. We show that making assumptions about causal mechanisms that link weather extremes and drought via agricultural collapse oversimplifies a complex system. The effects of a drought are not only determined by its severity in meteorological terms, but also by the ability of the affected agricultural system to recover. Furthermore, to understand the causal effects of droughts on conflict risk, we need to move closer to actual impacts on the ground, from broad-scale and distal meteorological drought proxies to data on agricultural productivity and its socioeconomic impacts. Temporally and spatially detailed data of sufficient quality are often challenging to acquire in areas affected by violent conflict. Here we propose a remote sensing approach focused on the intermediate variable in the climate-conflict nexus: agriculture.

By using longitudinal data on cropping and fallowness patterns, we provide insights into how the 2007–2009 meteorological drought affected the agricultural system in the short and long term. In particular, our dense time series revealed temporal dynamics that would have remained hidden in a setup of broader time steps. Existing products that consistently map dense time series of land cover change are often limited to forest cover[54] or have limitations in capturing the dynamics of active and fallow croplands[55]. Yet, consolidated image archives (i.e., MODIS, Landsat), new sensor constellations (Sentinel 1 and 2, Landsat 9) at no-cost availability, and increasing cloud-based computational capabilities[56] now allow for mapping agricultural land-use change at high spatial and/or temporal resolution back to the 1980s. This will allow for establishing a more robust and comprehensive link between meteorological droughts and agricultural activity than is currently done in most climate-conflict studies.

The "Syrian climate-conflict narrative" has received much attention in media and policy circles, and has become a frequent example of a "climate-induced conflict", despite the research community's more careful and nuanced conclusions[26,35,36]. With this study we wish to draw attention to the agricultural system as central for understanding drought vulnerability and the impacts of climate stress on societies. Knowing, for example, how cropland areas respond to drought and conflict is crucial for understanding where to focus resources to aid the population, as well as for post-conflict reconstruction. Regardless of the exact role of the 2007–2009 drought in the Syrian conflict, our research highlights the importance of building resilience to drought and climate stress in rural communities.

Methods

Cropland dynamics. For cropland extent, we use a land-use/land-cover dataset[49,57], which covers the area between 28.35-37.84°N and 35.29-49.14°E (Iraq and Syria) and shows annual cropland extent (single- and double cropping) as well as other land covers for the period 2000–2016 (Supplementary Table 1).

Classification method. Our classification of land-use/land-cover was based on an 8-day NDVI time series from MODIS Terra data, which we calculated from MODIS surface reflectance values (MOD09Q1)[58]. We smoothened the time series by applying a 30-day moving average to remove holes and pixels contaminated by clouds. Our underlying assumption for the analysis was that the different land-cover types in our study area show distinct phenological signals[59,60] (Supplementary Fig. 2).

We collected training samples from four different years (i.e., 2003, 2007, 2013, and 2015), determined by the availability of high-quality Landsat data. To find representative training samples, we used a combination of Landsat RGB composites and high-temporal resolution MODIS phenological profiles. We first visually identified a training location for our land cover class of interest (e.g., 'cropland (single)') in a Landsat composite (i.e., at 30 m resolution). To ensure that only clear training samples enter in our classification model we only selected samples that we covered by entire MODIS pixels. We then compared this location to the underlying phenological profile of our MODIS NDVI time series of the same year and labeled the training point in accordance with the phenological profile. We identified a total of 1573 training points across the four years (Supplementary Table 2), and we used these points as input for our classification.

We used the smoothed MODIS NDVI time series (i.e., 46 values per year), as well as a set of spectral-temporal metrics (20 in total, e.g., median-maximum ratio, mean, amplitude, etc.) as input (hereafter: NDVI collection). We used these input data to build a time-calibrated model using the random forest statistical technique. To do so, we extracted for each point of our training dataset the NDVI collection of the respective year (e.g., for a training point of the year 2007 the collection of the year 2007) and used this information to apply a two-stage classification approach. First, we parameterized a random forest model with 500 trees using all 66 input bands, ranked all bands based on their variable importance, and selected the 15 bands/metrics with the highest variable importance (Supplementary tble 3). Second, we used these 15 bands/metrics, parameterized a new random forest model, and used this model to predict our land cover classes for each year of our analysis (i.e., 2000–2016).

Fallowness data. To identify fallow areas, we defined a "normal cropland extent" based on the most frequent class (mode value) over the 2000–2016 period. We then defined "normal cropland" as where the most frequent class was either "single cropped" or "double cropped". For each year we compared this "normal cropland extent" to the actively cropped land to calculate the area that was fallow or inactive.

Collection of reference data and accuracy assessments. An accuracy assessment for the year 2014 was presented in Eklund et al.[49]. This was based on 800 random training points (roughly 200 points per class) for the year 2014 with a minimum distance of 500 meters between the validation points. The truth class of each of these points was determined by means of visual assessment of Landsat scenes and corresponding NDVI seasonality. The reason for choosing the year 2014 was data availability, as it was the first full year with data from Landsat 8. The overall accuracy for the 2014 classification was 80% with a producer accuracy of 95% and a user accuracy of 66% for single cropland (Supplementary Table 4). High-intensity cropland with two harvests showed a producer accuracy of 74% and a user accuracy of 92%. Other classes' accuracies were above 75%.

In addition to the validation for the year 2014, we independently validated the individual years that went into our classification. This enabled us to (a) assess the quality of each individual classification, and (b) to extract more robust area estimates with confidence intervals. We undertook the validation in two steps: first, we randomly sampled 1700 points (i.e., 100 per year) in areas of stable cropland. Second, we additionally sampled 1003 points (59 per year) in areas that had been fallow or inactive in at least one year during our study period, since change classes are often more error prone than stable land cover classes. We then manually assessed each point by visually interpreting the MODIS phenological evolution of the pixel, and by confirming our interpretation using Google Earth imagery. Once we labeled all classes, we generated an error matrix for each year, calculated the overall classification accuracy as well as class-wise user's and producer's accuracies, and calculated confidence intervals around our area estimates[61], following best practices[62]. Our results suggest highly accurate land-cover maps (Supplementary Table 5). On average, our annual fallow/cropland maps reached an average overall accuracy of 90% (Standard Deviation (SD) of 6%). User's and producer's accuracies were quite high, with 2016 showing the highest average user's accuracies (97%, SD of 9%) and the highest average producer's accuracy (97%, SD of 11%). The resulting confidence intervals around our area estimates were generally small except for 2001 (see Supplementary Table 5).

Effects of dryness on fallowness. The statistical analysis of the effect of dryness on fallowness uses 65 0.5° × 0.5° grid cells containing cropland (Supplementary Fig. 3), observed annually, with resolution corresponding to meteorological data from the Climatic Research Unit at the University of East Anglia (CRU) constituting the most fine-grained temperature *and* precipitation data available[63]. We use a unit fixed effects model since we are interested in the temporal variation within areas. We use a spatial lag model including a spatial lag of the independent variable (Spatial Durbin-model), using a maximum likelihood-estimator as this allows for endogenous effects between units[64]. The spatial Y accounts for simultaneous and reciprocal dynamics in which farmers in neighboring areas decide whether to crop or leave the land fallow, whereas the spatial lag of dryness captures spatial dependence in the observable sources of behavior that is not due to the diffusion captured by the spatial Y (see below and Supplementary Figs. 3 and 4 for a fuller elaboration)[65]. Our measure of dryness is the panel-standardized SPEI6-measure, which incorporates the combined effects of precipitation and temperature[66] during six months – in our case the months October–March. These months capture the rainy season prior to the main harvest (spring/summer). Fallowness is operationalized as the share of cropland in each grid-cell that are classified as bare soil in the year in question. Since most regression estimators have their weaknesses and the literature has not settled on whether time-fixed effects should be included, we report one specification with year dummies and one without. Additionally, we ran a host of alternative estimators, but our overall results did not change substantially from those reported in Fig. 3 (see Supplementary methods 1 and Supplementary Tables 7–22 for more details). Below, we specify the methods more in detail. For tests on the potential of armed conflict on increasing sensitivity to drought, as well as the link between fallowness and conflict, see Supplementary Method 1. Replication files for all analyses are available in Supplementary Data 3.

Study area. We estimate our model using grid cells with non-missing data as our unit of analysis. Out of 102 grid cells covering Syria, 65 have agricultural areas, while 37 cells are excluded as they do not contain detectable agricultural zones throughout the long-term period. This results in a time-series cross-section with 65 grid cells observed across 17 years (2000–2016) having at least one pixel of cropland (see Fig. S2). This results in 1,105 observations with variation on both the dependent and independent variable.

Cropland and Fallowness data. For our statistical analysis, we used the land use data described above and measured the share of cropland pixels that were fallow in a grid cell in each year. This enabled us to capture fallowness relative to the cell normal. Supplementary Fig. 3 shows fallowness patterns averaged by grid cell for 2008 (right panel).

Growing season drought. In order to capture the combined effect of precipitation and temperature on soil moisture, and therefore using a measure that closely resembles agricultural drought, we employ the Standardized Precipitation and Evapotranspiration Index (SPEI) based on data from the Climatic Research Unit of University of East Anglia CRU v.3.22, acquired through PRIO-GRID v. 2.0[67]. The SPEI index measures drought severity according to its intensity and duration and can identify the onset and end of drought episodes through both time and space. This index calculates the difference between the observed water balance by subtracting potential evapotranspiration (PET) from precipitation for the month in question. The calculation of PET is done according to the Penman-Monteith (PM) equation for calculating evapotranspiration, which captures the effect of solar radiation, temperature, wind speed, and relative humidity – if available[68]. Thereafter this monthly water balance is compared and standardized according to the long-term median water balance for that month and is, therefore, a more reliable measure of drought severity than a measure using rainfall alone, substantially better suited to capture the effect of global warming on agriculture. The original SPEI-variable has an average of 0 and a standard deviation of 1 for all units and is therefore comparable across units and within units over time.

Since the main share of the rainfall in Syria falls between October and March, and this, therefore, constitutes arguably the most crucial part of the growing season, we calculate and use a six months version of SPEI, calculated over the months October to March (SPEI-6). We then compared, SPEI6 for each year, to the mean of the same temporal interval in previous years. We calculate SPEI-values for October-December at year *t*-1 and January-March for year *t* and compare this to the normal using data from 1980-2010. For example, SPEI values combined from October to December of 2007 and January to March of 2008 constitutes our measure of drought when analyzing the effect of drought on fallowness for 2008.

Irrigation data. We generated our measure of irrigation in each grid cell using the AEI-EARTHSTAT_IR raster dataset which uses pixelated data on areas equipped for irrigation in year 1990[69]. First, we clipped the irrigation raster so that it intersects with agricultural areas, using information from the data on which areas could potentially be fallow, before we aggregated the mean raster value of irrigation within each grid cell. The resultant value captures the share of cropland in each cell that is irrigated, reflecting the importance of irrigation for agriculture in each cell. Supplementary Fig. 3 shows the irrigation data for agricultural areas in Syria.

Northern governorates. Since the Northern governorates of Deir ez-Zor, Aleppo, Raqqa and al-Hasakah (Fig. 1) are argued to have been particularly hard hit by the drought and government policies, we generated a dichotomous measure taking the value 1 for all cells that fell within these governorates and 0 otherwise.

Variable transformations. Since the spatial lag model using the maximum likelihood estimator is vulnerable to non-normally distributed variables[64], having variables that are not too far from being normally distributed is desirable. Our tests show that panel-demeaned fallowness and SPEI6-variables have only weak skewness and kurtosis, with transformations not improving fit. Since we rely on a unit fixed effects models, demeaning of the time-variant fallowness and SPEI6-variables is inbuilt in the algorithm, we used the raw data for SPEI6 and fallowness. As supplementary Tables 7 and 13 show, there is little difference between using raw data versus the panel demeaned-panel detrended fallowness and SPEI6-variables, and analyses comparing raw vs. panel-demeaned (not detrended) variables yield identical results (available on request). Since the irrigation variable has high kurtosis, and this is not demeaned, we took the square root of the variable. The resulting variable is closer to a normal distribution than the original. We interact this variable with the drought measure in order to capture the potentially different effect of drought in areas more vs. less reliant on irrigation.

Estimation strategy and sensitivity tests. In the subsequent analysis, we employ various conventional and novel statistical models. Each model explicitly states the model used for the estimation of the parameters. *OLS* refers to ordinary least squares, *logit* to logistic regression, and *nbreg* to negative binomial count models. The models where fallowness is the outcome we employ spatial fixed effects models as implemented through the *spxtregress* command in STATA.

We estimate panel grid-cell, fixed-effects models to exploit the variation in drought intensity and fallow cropland areas within the same grid cell over time. To minimize the impact of possible unobserved confounders, this model effectively accounts for all time-invariant heterogeneity, making us able to account for time-invariant omitted variables.

Since our data consists of contiguous subnational units, spatial dependence should be accounted for. We tested the Moran's I for fallow land using annual cross-sections of grid-cells in Syria (Moran's I is calculated on cross-sectional data). Supplementary Fig. 4 shows significant clustering of fallow land in 2000, 2007–2009 period and 2014, all of which are years that experienced droughts. This suggests that fallow land tends to be more clustered in years of drought than in relatively normal years. Clearly, our data exhibit significant spatial autocorrelation (for most years), and this needs to be accounted for in the models, motivating the use of spatial regression modeling.

The significant spatial clustering in fallowness reflects diffusion in cropping strategies. To account for such interdependencies, we estimate spatial regression models when analyzing whether there was a structural break in agriculture's sensitivity to drought. Since the formal tests distinguishing between different spatial modeling strategies generally have weak test power, with alternative models not nested in each other, expectations about mechanisms guide the choice of estimation strategy[70]. We expect farmers in proximate units to communicate and adapt to each other's cropping strategies. Knowledge about other farmers abandoning their crops can trigger neighboring farmers to do the same. Since this is a simultaneous and reciprocal dynamic in which learning goes both ways and occurs within the same growing year, a spatial lag model is preferable to a spatial error model, since the former can account for reciprocity and therefore avoid simultaneity bias using the Maximum Likelihood estimator. Since there is also spatial clustering in our drought measure, we also included a spatial lagged variable of the SPEI6 measure. Accounting for spatial dynamics in general yields more conservative standard errors compared to a conventional unit fixed effects (non-spatial) model (results available on request).

Since we are interested in the potential different effects between the pre (2000-07) and post (2008-16) drought period, we relied on models with and without year fixed-effects, since STATA's supporting material and communication is unclear on whether or not variables that are time-variant but static across all observations in the same cross-section can be used. We did not use temporally lagged dependent variables in the models reported in Fig. 3 as this introduces Nickell bias in fixed-effects models[71], and one should generally be careful when considering using them in spatial models[72,73]. The models behind the results reported in Fig. 3 are reported in Supplementary Tables 7–12.

Analyzing panel-wise detrended data. In sensitivity tests (Supplementary Tables 13–14), we account for that our SPEI6 and fallowness data show mild symptoms of trending. We first performed panelwise linear detrending of these two variables by conducting cell-wise regression of each variable using time as the explanatory variable. The residuals from these models constitute detrended variables, which we used to rerun our models with, both without (Supplementary Table 13) and with time fixed effects (Supplementary Table 14). In these models, any cell-specific temporal linear trend is taken out of the data. The results corroborate the main results. The results for detrended analyses without year fixed effects are very similar to the parallel model without detrended variables (compare Supplementary Tables 13 and 7). There is only a modestly higher difference when comparing the models using detrended vs. non-detrended variables when applying year fixed effects (compare Supplementary Tables 14 and 8).

Excluding cases with very few pixels of cropland. The main models include all cells with non-zero pixels of cropland. In order to ensure that our results are not driven by such outliers, we ran our main models excluding the three out of 65 cases with the least cropland, since these three cases have substantially less cropland than the other cells. Comparing our overall models without year fixed effects with the parallel models without these three outliers shows a slight drop in the effect of drought on fallowness (see Tables S7 and S15). For the models using time fixed effects, the models with all cells (Supplementary Table 8) and those without the three with least agricultural land (Supplementary Table 16) are also very similar, without any systematic and substantial change in results. We also tested effects without the ten cells with the least cropland, which generally reduced the effect of drought on fallowness for all models, but, crucially, the difference between time-periods remained similar. However, this accounts for 10 out of 65 cells, which reduces the sample considerably, and it also breaks up the spatial contiguity matrix making the results less reliable.

Results including a temporally lagged dependent variable. In addition to running analyses with and without year fixed effects, and with and without detrended variables, we conducted a final sensitivity analysis to root out any potential temporal dependence. This was done by including a temporally lagged dependent variable in our core models. Some caution should be applied when interpreting fixed effects models with a lagged dependent variable as they can suffer from the so-called Nickell bias[74], essentially, with very little residual variation in the dependent variable being left for the causal variables to pick up. Comparing our core model without year fixed effects with the parallel model with a lagged dependent variable; we see that the effect of SPEI6 on fallowness is slightly weakened in the latter type of models. The results for our core models including time fixed effects are also slightly weakened when including a lagged dependent variable (compare Supplementary Tables 8 and 18). A slight weakening of effects is expected when combining unit fixed effects and a lagged dependent variable[74], and while remedies have been suggested, no clear solution is available[71,73]. The slight decrease in effect for the models including a lagged dependent variable could also be due to the models in Supplementary Table 17 also excluding the year 2000 which was very dry and saw substantial fallowness.

Further sensitivity analyses were run but not shown here for space constraints. These are available upon request.

Data availability

The land use datasets generated during and/or analysed during the current study are available in the Zenodo repository, https://doi.org/10.5281/zenodo.4224925. SPEI and Irrigation data is available through PRIO-GRID: https://grid.prio.org/#/. Data used in the graphs in Figs. 2 and 3 are provided as Supplementary Data.

Code availability

Replication files for the STATA 17.0 Standard Edition analysis are available as Supplementary data.

Received: 26 March 2021; Accepted: 23 February 2022;
Published online: 06 April 2022

References

1. Adger, W. N. et al. Chapter 12: Human security. in Climate Change 2014: Impacts, Adaptation, and Vulnerability. Part A: Global and Sectoral Aspects. Contribution of Working Group II to the Fifth Assessment Report of the IntergovernmentalPanel on Climate Change 37 (2014).
2. Gleditsch, N. P. & Nordås, R. Conflicting messages? The IPCC on conflict and human security. *Political Geography* **43**, 82–90 (2014).
3. Schleussner, C.-F., Donges, J. F., Donner, R. V. & Schellnhuber, H. J. Armed-conflict risks enhanced by climate-related disasters in ethnically fractionalized countries. *Proc. Natl. Acad. Sci. USA* **113**, 9216–9221 (2016).
4. Buhaug, H., Croicu, M., Fjelde, H. & von Uexkull, N. A conditional model of local income shock and civil conflict. *J. Politics* **83**, 354–366 (2020).
5. Bernauer, T., Böhmelt, T. & Koubi, V. Environmental changes and violent conflict. *Env. Res. Lett.* **7**, 015601 (2012).
6. Koubi, V. Climate Change and Conflict. *Annu. Rev. Polit. Sci.* **20**, 343–360 (2019).
7. Jerven, M. *Poor numbers: how we are misled by African development statistics and what to do about it*. (Cornell University Press, 2013).
8. Theisen, O. M., Holtermann, H. & Buhaug, H. Climate wars? Assessing the claim that drought breeds conflict. *Int. Security* **36**, 79–106 (2012).
9. Koren, O. Food abundance and violent conflict in Africa. *Am. J. Agric. Econ.* **100**, 981–1006 (2018).
10. Caruso, R., Petrarca, I. & Ricciuti, R. Climate change, rice crops, and violence: Evidence from Indonesia. *J. Peace Res.* **53**, 66–83 (2016).
11. Sarsons, H. Rainfall and conflict: A cautionary tale. *J. Dev. Econ.* **115**, 62–72 (2015).
12. Bergholt, D. & Lujala, P. Climate-related natural disasters, economic growth, and armed civil conflict. *J. Peace Res.* **49**, 147–162 (2012).
13. Buhaug, H. Climate not to blame for African civil wars. *Proc. Natl. Acad. Sci.* **107**, 16477–16482 (2010).
14. Buhaug, H., Benjaminsen, T. A., Sjaastad, E. & Magnus Theisen, O. Climate variability, food production shocks, and violent conflict in Sub-Saharan Africa. *Envi. Res. Lett.* **10**, 125015 (2015).
15. Buhaug, H. et al. One effect to rule them all? A comment on climate and conflict. *Clim. Change* **127**, 391–397 (2014).
16. Burke, M. B., Miguel, E., Satyanath, S., Dykema, J. A. & Lobell, D. B. Warming increases the risk of civil war in Africa. *Proc. Natl. Acad Sci.* **106**, 20670–20674 (2009).
17. Hsiang, S. M., Burke, M. & Miguel, E. Quantifying the Influence of Climate on Human Conflict. *Science* **341**, 1235367–1235367 (2013).
18. Salehyan, I. Climate change and conflict: Making sense of disparate findings. *Polit. Geogr.* **43**, 1–5 (2014).
19. von Uexkull, N., Croicu, M., Fjelde, H. & Buhaug, H. Civil conflict sensitivity to growing-season drought. *Proc. Natl. Acad. Sci.***113**, 12391–12396 (2016).
20. Zhang, D. D. et al. The causality analysis of climate change and large-scale human crisis. *Proc. Natl. Acad. Sci.* **108**, 17296–17301 (2011).
21. Adams, C., Ide, T., Barnett, J. & Detges, A. Sampling bias in climate–conflict research. *Nat. Clim. Change* **8**, 200–203 (2018).
22. Raleigh, C., Linke, A. & O'Loughlin, J. Extreme temperatures and violence. *Nat. Clim. Change* **4**, 76–77 (2014).
23. Gleick, P. H. Water, Drought, Climate Change, and Conflict in Syria. *Wea. Climate Soc.* **6**, 331–340 (2014).
24. Kelley, C. P., Mohtadi, S., Cane, M. A., Seager, R. & Kushnir, Y. Climate change in the Fertile Crescent and implications of the recent Syrian drought. *Proc. Natl. Acad. Sci.* **112**, 3241–3246 (2015).
25. Werrell, C. E., Femia, F. & Sternberg, T. Did We See It Coming?: State Fragility, Climate Vulnerability, and the Uprisings in Syria and Egypt. *SAIS Rev. Int. Aff.* **35**, 29–46 (2015).
26. De Châtel, F. The Role of Drought and Climate Change in the Syrian Uprising: Untangling the Triggers of the Revolution. *Middle Eastern Studies* **50**, 521–535 (2014).
27. Hoffmann, C. Environmental determinism as Orientalism: The geo-political ecology of crisis in the Middle East. *J. Hist. Sociol.* **31**, 94–104 (2018).
28. Daoudy, M. *The Origins of the Syrian Conflict: Climate Change and Human Security*. (Cambridge University Press, 2020).
29. Ide, T. Climate War in the Middle East? Drought, the Syrian Civil War and the State of Climate-Conflict Research. *Curr. Clim. Change Rep.* **4**, 347–354 (2018).
30. Feitelson, E. & Tubi, A. A main driver or an intermediate variable? Climate change, water and security in the Middle East. *Global Env. Change* **44**, 39–48 (2017).
31. Werrell, E. C. E. & Femia, F. The Arab Spring and Climate Change. 68 (2012).
32. Integrated Regional Information Networks (IRIN). Syria: Drought response faces funding shortfall. irinnews.org/report/87165/syriadrought-response-faces-funding-shortfall (2009).
33. Solh, M. Tackling the drought in Syria. *Nat. Middle East*. https://www.natureasia.com/en/nmiddleeast/article/10.1038/nmiddleeast.2010.206 (2010).
34. Ash, K. & Obradovich, N. Climatic Stress, Internal Migration, and Syrian Civil War Onset. *J. Conflict Resolut.* **64**, 3–31 (2020).
35. Eklund, L. & Thompson, D. Differences in resource management affects drought vulnerability across the borders between Iraq, Syria, and Turkey. Ecol. Soc. **22**, (2017).
36. Selby, J., Dahi, O. S., Fröhlich, C. & Hulme, M. Climate change and the Syrian civil war revisited. *Polit. Geogr.* **60**, 232–244 (2017).
37. Fröhlich, C. J. Climate migrants as protestors? Dispelling misconceptions about global environmental change in pre-revolutionary Syria. *Contemp. Levant* **1**, 38–50 (2016).
38. Selby, J. Climate change and the Syrian civil war, Part II: The Jazira's agrarian crisis. Geoforum https://doi.org/10.1016/j.geoforum.2018.06.010 (2018).
39. Gürcan, E. C. Extractivism, Neoliberalism, and the Environment: Revisiting the Syrian Conflict from an Ecological Justice Perspective. *Cap. Nat. Social.* **30**, 91–109 (2019).
40. Ababsa, M. The End of a World Drought and Agrarian Transformation in Northeast Syria (2007–2010). *Polit. Econ Int.* **1**, 199e222 (2015).
41. Fraser, E. D. G. & Stringer, L. C. Explaining agricultural collapse: Macro-forces, micro-crises and the emergence of land use vulnerability in southern Romania. *Global Env.Change* **19**, 45–53 (2009).
42. Cumming, G. S. & Peterson, G. D. Unifying research on social–ecological resilience and collapse. *Trend Ecol. Evol.* **32**, 695–713 (2017).
43. Walker, B., Holling, C. S., Carpenter, S. R. & Kinzig, A. P. Resilience, Adaptability and Transformability in Social-ecological Systems. *Ecol. Soc.* **9**, art5 (2004).
44. Gleick, P. H. Climate, water, and conflict: Commentary on Selby et al. 2017. *Polit. Geogr.* **60**, 248–250 (2017).
45. Hendrix, C. S. A comment on "climate change and the Syrian civil war revisited". *Polit. Geogr.* **60**, 251–252 (2017).
46. Kelley, C., Mohtadi, S., Cane, M., Seager, R. & Kushnir, Y. Commentary on the Syria case: Climate as a contributing factor. *Polit. Geogr.* **60**, 245–247 (2017).
47. Estel, S., Kuemmerle, T., Levers, C., Baumann, M. & Hostert, P. Mapping cropland-use intensity across Europe using MODIS NDVI time series. *Env. Res. Lett.* **11**, 024015 (2016).
48. Food and Agriculture Organization of the United Nations (FAO). FAOSTAT: Crops and livestock products. https://www.fao.org/faostat/en/#data/QCL.
49. Eklund, L., Degerald, M., Brandt, M., Prishchepov, A. V. & Pilesjö, P. How conflict affects land use: agricultural activity in areas seized by the Islamic State. *Environ. Res. Lett.* **12**, 054004 (2017).
50. Cattaneo, C. et al. Human Migration in the Era of Climate Change. *Rev. Env. Econ. Policy* **13**, 189–206 (2019).
51. Nawrotzki, R. J. & Bakhtsiyarava, M. International Climate Migration: Evidence for the Climate Inhibitor Mechanism and the Agricultural Pathway: Evidence for the Climate Inhibitor Mechanism and the Agricultural Pathway. *Population, Space and Place* **23**, e2033 (2017).
52. De Longueville, F. et al. Comparing climate change perceptions and meteorological data in rural West Africa to improve the understanding of household decisions to migrate. *Clim. Change* https://doi.org/10.1007/s10584-020-02704-7 (2020).
53. UN-OCHA. SYRIA DROUGHT RESPONSE PLAN. 50 http://www.unocha.org/cap/appeals/drought-response-plan-syria-2009 (2009).
54. Hansen, M. C. et al. High-Resolution Global Maps of 21st-Century Forest Cover Change. *Science* **342**, 850 (2013).
55. Friedl, M. A. et al. MODIS Collection 5 global land cover: Algorithm refinements and characterization of new datasets. *Remote Sens. Environ.* **114**, 168–182 (2010).
56. Gorelick, N. et al. Google Earth Engine: Planetary-scale geospatial analysis for everyone. *Remote Sens. Environ.* **202**, 18–27 (2017).
57. Eklund, L., Brandt, M. & Prishchepov, A. V. Land use/land cover in Iraq and Syria, 2000–2016. https://doi.org/10.5281/zenodo.4224926 (2020).
58. Vermote, E., Kotchenova, S. & Ray, J. MODIS surface reflectance user's guide. MODIS Land Surface Reflectance Science Computing Facility, version **1**, 1–40 (2011).
59. Pittman, K., Hansen, M. C., Becker-Reshef, I., Potapov, P. V. & Justice, C. O. Estimating global cropland extent with multi-year MODIS data. *Remote Sens.* **2**, 1844–1863 (2010).
60. Eklund, L., Persson, A. & Pilesjö, P. Cropland changes in times of conflict, reconstruction, and economic development in Iraqi Kurdistan. *Ambio* **45**, 78–88 (2016).
61. Stehman, S. V. Estimating area from an accuracy assessment error matrix. *Remote Sens. Environ.* **132**, 202–211 (2013).

62. Olofsson, P. et al. Good practices for estimating area and assessing accuracy of land change. *Remote Sens. Environ.* **148**, 42–57 (2014).
63. Harris, I., Osborn, T. J., Jones, P. & Lister, D. Version 4 of the CRU TS monthly high-resolution gridded multivariate climate dataset. *Scientific data* **7**, 1–18 (2020).
64. Ward, M. & Gleditsch, K. Spatial Regression Models. https://doi.org/10.4135/9781412985888 (Sage, 2008).
65. Salima, B. A., Le Gallo, J. & Védrine, L. Chapter 7: Spatial econometrics on panel data. in Handbook of Spatial Analysis: Theory and Application with R 179–203 (Institut national de la statistique et des études économiques (INSEE), 2018).
66. Beguería, S., Vicente-Serrano, S. M. & Angulo-Martínez, M. A multiscalar global drought dataset: the SPEIbase: a new gridded product for the analysis of drought variability and impacts. *Bull. Am. Meteorol. Society* **91**, 1351–1356 (2010).
67. Tollefsen, A. F., Strand, H. & Buhaug, H. PRIO-GRID: A unified spatial data structure. *J. Peace Res.* **49**, 363–374 (2012).
68. Beguería, S., Vicente-Serrano, S. M., Reig, F. & Latorre, B. Standardized precipitation evapotranspiration index (SPEI) revisited: parameter fitting, evapotranspiration models, tools, datasets and drought monitoring. *Int. J. Climatol.* **34**, 3001–3023 (2014).
69. Siebert, S. et al. Historical irrigation dataset (HID). *Hydrolo. Earth Syst. Sci.* **19**, 1521–1545 (2015).
70. Ward, M. D. & Gleditsch, K. S. *An introduction to spatial regression models in the social sciences.* (Ward & Kristian Skrede Gleditsch, 2007).
71. Angrist, J. D. & Pischke, J.-S. Mostly harmless econometrics: An empiricist's companion. (Princeton university press, 2008).
72. Franzese, R. J. & Hays, J. C. *Empirical modeling of spatial interdependence in time-series cross-sections. in Methoden der vergleichenden Politik-und Sozialwissenschaft* 233–261 (Springer, 2009).
73. Plümper, T. & Neumayer, E. Model specification in the analysis of spatial dependence. *Eur. J. Polit. Res.* **49**, 418–442 (2010).
74. Nickell, S. Biases in dynamic models with fixed effects. Econometrica. *J. Econ. Society* 1417–1426 (1981).

Acknowledgements
This research was conducted as part of the Middle East in the Contemporary World (MECW) project funded by Vetenskapsrådet, and the project Climate Stress in Syria, funded by Svenska Forskningsrådet Formas (grant 2019-01131). Theisen and Tollefsen's work was funded by the European Research Council, Climate Variability and Security Threats (CLIMSEC, grant 648291).

Author contributions
L.E. led the writing of the manuscript, carried out the land-use analysis and classification evaluation, and prepared figures for the manuscript. O.M.T. contributed to the research design, the writing of the manuscript, carried out the statistical analysis and aided with the figure design. M.B. contributed to the writing of the manuscript, and aided with the classification evaluation and figure design. A.F.T. aided with the statistical analysis and data for the figures. T.K. aided with the research design, contributed to the writing of the manuscript and the figure design. J.Ø.N. aided with the research design and contributed to the writing of the manuscript.

Funding
Open access funding provided by Lund University.

Competing interests
The authors declare no competing interests.

Additional information
Supplementary information The online version contains supplementary material available at https://doi.org/10.1038/s43247-022-00405-w.

Correspondence and requests for materials should be addressed to Lina Eklund.

Peer review information *Communications Earth & Environment* thanks Ore Koren and the other, anonymous, reviewer(s) for their contribution to the peer review of this work. Primary Handling Editors: Clare Davis. Peer reviewer reports are available.

Reprints and permission information is available at http://www.nature.com/reprints

Publisher's note Springer Nature remains neutral with regard to jurisdictional claims in published maps and institutional affiliations.